OFDM (DMT) Bit and Power Loading for Unequal Error Protection

Werner Henkel and Khaled Hassan
School of Engineering and Science, International University Bremen
28759 Bremen, Germany, {w.henkel & k.hassan}@iu-bremen.de

***Abstract*— This paper proposes an algorithm that distributes bits according to different noise margin levels, thereby realizing unequal error protection (UEP). The new approach is based on a non-UEP allocation algorithm by Chow, Cioffi, and Bingham. The new algorithm is designed to be robust to non-stationary impulse noise and channel variations by integrating a new SNR-sorting scheme. Simulation results show that the highly protected bits are spread over a high number of carriers at low SNR, thereby ensuring that SNR variations due to non-stationary noise will not influence these carriers much. Additionally, narrow-band interference will not hit a large amount of important data.**

***Index Terms*— OFDM, DMT, UEP, bit loading, bit allocation, power loading, power allocation**

I. Introduction

THE concept of multicarrier modulation (MCM) is increasingly adopted to current transmission systems due to its flexibility. Orthogonal frequency division multiplexing (OFDM) is the passband form of MCM used in wireless systems. The baseband form of MCM is discrete multitone (DMT), which is widely used in wireline applications such as asymmetric digital subscriber line (ADSL) and very-high-bit-rate DSL (VDSL). Unlike single-carrier modulation which assigns the whole resource to one carrier, MCM divides the available bandwidth into N subcarriers. The number of bits per subcarrier is adaptively tuned , such that subcarriers with high signal-to-noise ratios are loaded with a high number of bits. This process is called *bit-loading*.

Bit-loading has been investigated mainly for DMT systems. A number of algorithms has been proposed to solve the bit-loading problem in the DSL environment. The optimal solution for the discrete bit-loading has been proposed by Hughes-Hartogs [1] as a greedy iterative algorithm, successively allocating bits to subcarriers that require the minimum incremental power until either the total power exceeds the maximum power or the target rate is reached. Later, Campello [2] has studied an optimal discrete algorithm based on [1] but with a faster implementation. The main optimization problem in this algorithm is to find groups of subcarriers with the same bit-loading values, adaptively changing the number of bits until the minimum power is achieved. Sub-optimal solutions were proposed to reduce the complexity. Based on Shannon's capacity formula, Chow, Cioffi, and Bingham proposed a sub-optimal algorithm [3] that loads the subcarriers according to the channel capacity for a certain noise margin, γ_m. Furthermore, γ_m is adaptively changed to achieve a required maximum number of bits. In [3], the power is allocated after the bits have been loaded, which leaves no room for further optimization. Fischer and Huber have proposed another sub-optimal algorithm [4] that allocates the bits and the power jointly. The derivation of the algorithm is based on Lagrange multipliers and minimizes the symbol-error probability.

All the previous loading algorithms achieve a constant error probability, which is not really required for many applications like video and audio. Such source encoded data requires to be protected according to its importance, i.e., parts of the data (like header and near DC components) need more protection than others. Unequal error protection (UEP) channel coding would be one possible solution together with the current loading algorithms. However, the physical transport already allows for an easy implementation of UEP properties that can reduce the effort and the redundancy bits in channel coding. Especially, when using OFDM (DMT), the bit-loading process can be controlled to realize unequal protection. We propose an iterative algorithm realizing different noise margins γ_j for priority classes j as a modification of the bit-loading scheme by Chow, Cioffi, and Bingham [3] often applied in current equal protecting (non-UEP) multicarrier implementations. To the knowledge of the authors, there is currently only one already published UEP loading scheme by Yu and Wilson [5] based on the non-UEP loading algorithm by Fischer and Huber [4]. It requires lengthy iterations and will fail in case of non-stationary noise not taken into account during bit-allocation. Our algorithm proposes an SNR-sorting that ensures higher protection for the important data even under adverse non-stationary noise conditions. The rest of the paper is organized as follows: Section 2 states the proposed bit-loading algorithm. Section 3 describes the UEP bit-loading principle. Section 4 introduces the channel model. Section 5 discusses some simulation results. Finally, the paper in concluded with Section 6.

II. UEP: New Bit-Loading Principle

A. Bit-Rate Maximization

In this work, it is assumed to require a maximum target bit-rate B_T and individual target rates T_j for each priority class j such that

$$B_T \leq \sum_{j=0}^{N_g-1} T_j \ , \tag{1}$$

where N_g is the number of priority classes. A different noise margin γ_j is devoted to each priority class. Without loss of generality, the γ_j are assumed to have constant spacing. In order to satisfy the maximum target rate B_T, a bit-rate maximization problem (BRMP) is assumed as a starting point. Other formulations will be considered in future works. BRMP is described as follows

$$\max_{b \in Z} \left\{ B_{\text{tot}} = \sum_{k=0}^{N-1} b_k \right\} \tag{2}$$

subject to

$$\sum_{k=0}^{N-1} P_k(b_k) < P_T \ , \tag{3}$$

where B_{tot} is the total number of loaded bits, P_k is the power for the k^{th} subcarrier that is assigned to b_k bits, and N is the number of subcarriers.

B. SNR-Sorting

In order to realize UEP classes, SNR ranges have to be allocated to the required protection levels, N_g. This can be achieved by setting hypothetical SNR thresholds, τ_j, where the UEP requirements are fulfilled by modifying these thresholds, thereby changing the number of subcarriers for each class. In a way, this already defines a new sorting scheme, which we denote SNR-sorting. In practice, the carriers will initially be ordered according to the SNRs before introducing thresholds. SNR-sorting allocates the most important data with the higher γ_j to subcarriers with the lowest SNR and the least important data to subcarriers with the highest SNR. Allocating important data to the weaker subcarriers will protect these against non-stationary noise, as the SNR may not vary much. Another exploited advantage from combining such SNR-sorting and the UEP bit-loading, is spreading the important data over many subcarriers. This results in reducing the impact of harmful narrow-band interference. The opposite scheme, when the most important data are allocated to the subcarriers with the highest SNR, is in this paper referred to as 'inverse SNR-sorting'.

Figure 1 models a special case of three protection classes (Class_0, Class_1, and Class_2), where Class_0 is the highest protected class in both schemes.

III. The New UEP Bit and Power Loading Algorithm

The algorithm by Chow, Cioffi, and Bingham [3] is based on a modified Shannon capacity. It uses an adaptive noise-margin to fulfill the target rate. We also use margins γ_j for the different priority classes. Hence, the algorithm uses the rate relation

$$b_{k,j} = \log_2\left(1 + \frac{\text{SNR}_{k,j}}{\gamma_j}\right)$$

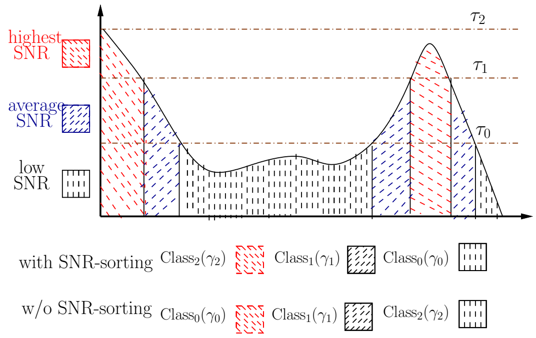

Fig. 1. SNR thresholds for different sorting schemes

$$\hat{b}_{k,j} = \begin{cases} \lfloor b_{k,j} + 0.5 \rfloor, & \text{if } b_{k,j} \leq b_{max} \\ b_{max}, & \text{if } b_{k,j} > b_{max} \end{cases}$$

$$\Delta b_{k,j} = b_{k,j} - \hat{b}_{k,j} \ , \tag{4}$$

where $b_{k,j}$ is the bit rate for the k^{th} carrier in the j^{th} priority class, such that, e.g., $j \in [0, \dots, N_g - 1]$ would correspond to N_g protection levels. γ_j is fixed for a set of carriers $k \in \mathcal{M}_j$. The number of bits, $b_{k,j}$ are truncated to the nearest integer $\hat{b}_{k,j}$, where $\Delta b_{k,j}$ is the 'quantization error', and b_{max} are the maximum allowed bits per subcarrier. Each group is composed of a certain number of bits, T_j, and the total target bit-rate is given by $B_T = \sum_{j=0}^{N_g-1} T_j$. We consider constant noise margin steps $\Delta\gamma_j$ between the groups. A generalization to different step sizes is obvious.

The complete algorithm is the following:

UEP Bit-Rate Maximization Algorithm
Input: $\text{SNR}_{k,j}$ in k^{th} subcarrier of j^{th} class, N, N_g, B_T, T_j, and $\Delta\gamma$
Output: γ_j, average probability of error $\hat{\mathcal{P}}_{ej}$, and bit allocation

1) transmitter sorts the subcarriers positions in case of "SNR-sorting".
2) ordered subcarrier indices are stored in the set $\mathcal{M}_j$, where $j \in [0, \cdots, N_g - 1]$
3) γ_0 may initially be set to 1 and is iteratively adjusted to fulfill the UEP requirements and the required individual number of bits T_j. Let γ_0 denote the highest protection level. The others are computed as $\gamma_j = \gamma_0 - j \cdot \Delta\gamma$ in dB
4) $b_{k,j}$ is calculated using (4), then number of subcarriers in $\mathcal{M}_j$, $j = 0, \dots, N_g - 2$ is adjusted iteratively using a binary search as described in Appendix A. This process is equivalent to sliding the SNR thresholds, τ_j.
5) If the overall bit rate B_{tot} is not equal to the target bit rate B_T, γ_0 is recalculated using the following adjustment, as in [3], $\gamma_{0,new} = \gamma_{0,old} \cdot 2^{\frac{B_{tot} - B_T}{N}}$ and γ_j, $j > 0$ are again calculated as in Step 3). Then, go to Step 4).

6) Else, if B_T is fulfilled and/or the maximum iteration count is reached, go to Step 7)
7) If the maximum number of iterations is approached without achieving B_T, brute-force measures, as in Step 8) and Step 9) of [3], are taken. Dependent on $\Delta b_{k,N_g-1}$ bits are added to the least protected class at locations of maximum $\Delta b_{k,N_g-1}$ or bits are removed at locations of minimum $\Delta b_{k,N_g-1}$ until the target bit-rate is fulfilled.
8) The power is allocated using the symbol-error rate equations in [6] and the modified ones in Appendix B, such that the power for each subcarrier is a function of the noise power at each subcarrier $N_{k,j}$, the rounded number of bits $\hat{b}_{k,j}$, and the required average error probability $\overline{\mathcal{P}}^e_M(\gamma_j)$ for the j^{th} class. This is performed using the following steps:

- As in Appendix B, the symbol-error probability under AWGN as a function of γ_j and $\hat{b}_{k,j}$ is

$$\mathcal{P}^e_M(\gamma_j, \hat{b}_{k,j}) = \left(1 - \frac{1}{\sqrt{2^{\hat{b}_{k,j}}}}\right) \operatorname{erfc}\left(\sqrt{\frac{3\gamma_j}{2}}\right) \cdot \left[2 - \left(1 - \frac{1}{\sqrt{2^{\hat{b}_{k,j}}}}\right) \operatorname{erfc}\left(\sqrt{\frac{3\gamma_j}{2}}\right)\right], \quad (5)$$

and the average error probability for each class is given by

$$\overline{\mathcal{P}}^e_M(\gamma_j) = \frac{1}{|\mathcal{M}_j|} \sum_{k \in \mathcal{M}_j} \mathcal{P}^e_M(\gamma_j, \hat{b}_{k,j}) \quad (6)$$

- as in [5], the power allocation, as a function of $\overline{\mathcal{P}}^e_M(\gamma_j)$, is given by

$$P_{k,j} = \frac{2N_k(2^{\hat{b}_{k,j}} - 1)}{3} \cdot \left[\operatorname{erfc}^{-1}\left(\frac{\overline{\mathcal{P}}^e_M(\gamma_j)\sqrt{2^{\hat{b}_{k,j}}}}{2\left(\sqrt{2^{\hat{b}_{k,j}}} - 1\right)}\right)\right]^2 \quad (7)$$

where $P_{k,j}$ and N_k are the signal power and noise energy, respectively.

IV. Channel Model

A. Cable Transfer Function

For numerical results, ADSL2*plus* with 512 subcarriers [7] is considered using an Austrian 0.4-mm cable of length 2 km. Wireline channels are mainly characterized by propagation losses and linear distortions. The so-called MAR 1 model was first introduce by Mossun in [8]. It is selected because of its causal time-domain impulse response.

The serial impedance Z_s and shunt admittance Y_p for the MAR 1 model is given by [9]:

$$Z_s = j2\pi f L_\infty + R_0 \left(\frac{1}{4} + \frac{3}{4}\sqrt{1 + \frac{as(f)(s(f)+b)}{(s(f)+c)}}\right),$$

$$Y_p = 2\pi f C_f \cdot (j + \tan(\delta)) = 2\pi f C_{1\mathrm{MHZ}} \cdot (jf/10^6)^{\frac{-2\delta}{\pi}},$$

$s(f) = \frac{\mu_0 jf}{0.75^2 R_0} \approx \frac{jf}{447.6R_0}$, $\mu_0 = 4\pi 10^{-4}$[H/km].
The approximated seven MAR 1 model parameters for an exemplary Austrian 0.4-mm cable are given in Table I.

TABLE I
MAR 1 MODEL PARAMETERS FOR 0.4 MM AUSTRIAN CABLE

	Definition	Value	Unit
R_0	DC resistance	291.973	[Ω/km]
L_∞	high freq. inductance	$6.3715 \cdot 10^{-4}$	[H/km]
a	Proximity factor	1.37005	const.
b	Proximity factor	$1.12015 \cdot 10^{-14}$	const.
c	Proximity factor	0.161583	const.
δ	shunt-capacity loss angle	0.0058163	const.
$C_{1\mathrm{MHz}}$	capacitance	$3.42986 \cdot 10^{-8}$	[F/km]

B. Additive Disturbances

1) Stationary Noise: In ADSL, a major impairment would be near-end crosstalk (NEXT). For numerical results, a combination of 10 T1 and 10 HDSL NEXT disturbers is assumed as stationary noise, additionally constant −130 dBm/Hz white Gaussian noise (AWGN). The approximated T1 and HDSL power spectrum densities (PSD) and their induced NEXT are given in [10].

2) Non-stationary Impulse Noise: Non-stationary impulse noise is a long noticed disturbance that has been analyzed for xDSL systems, e.g., in [11]. In this paper, real measured impulses are used. Figure 2 shows the relation between the background noise (from 10 T1 and 10 HDSL NEXT disturbers combination), the impulse noise, and the combination of both.

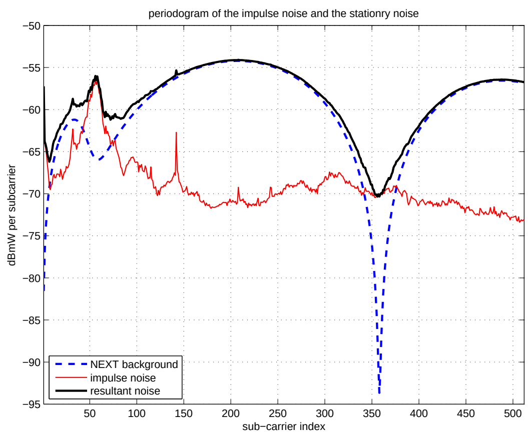

Fig. 2. Stationary background noise PSD from NEXT signals and pseudo-PSD of the impulse noise that is calculated as the average of squared FFT components of impulses

V. Simulation Results and Discussions

Our results are generated assuming an application that only requires three different protection classes. Each class requires different target-rates, T_j, and a fixed noise margin step size, $\Delta\gamma$, between these classes. $\Delta\gamma$ needs to be selected according to application requirements, and here it is assumed to be fixed at 3 dB. Thus, the symbol-error rate curves would be separated by 3 dB. The pure Chow-Cioffi algorithm [3] without UEP (non-UEP) bit-loading is chosen as a reference.

A. UEP Performance: SER Analysis

In this paper, SNR-sorting is an additional ingredient which has not been taken into account in [5]. Otherwise, high protected data will be extremely vulnerable to non-stationary channel conditions, like impulse noise and fast fading. However, there is a price to be payed if SNR-sorting is blindly applied. In order to study these effects more, we subdivide the analysis into two independent studies:

1) Channel with stationary noise only: Figure 3 shows the effect of stationary background noise for both sorting schemes, with and without SNR-sorting. All the curves show the desired spacing of 3 dB. Furthermore, we added the corresponding performance curve for non-UEP bit allocation. As expected, this curve represents an average performance relative to the UEP curves.

From Fig. 3, we see that there is a drawback when blindly applying SNR-sorting. SNR-sorting shows a worse performance in a stationary environment by almost 1.7 dB. This is due to the large quantization steps in power needed for allocating bits. This may result in having quite some non-used subcarriers at low SNRs, since these subcarriers were only devoted to high-priority bits, which cannot be placed there any more. One could allow for mixed allocation of additional lower priority bits on these unused low-SNR subcarriers. One could even go for mixed loading also for other subcarriers leading to hierarchical modulation formats at low-SNR carriers.4066086687350

2) Channel with impulse noise and stationary background noise: In this work, we studied real measured impulse noise. In order to compute a pseudo PSD, the frequency domain of the impulse noise signal was calculated by an FFT assuming it to be a stationary event, which is, of course, not true. Figure 4 shows the symbol-error rate curves due to impulse noise plus stationary noise. In this case, the system with SNR-sorting performs dramatically better than the inverse SNR-sorting. It can also be shown that inverse SNR-sorting, performances are even turned around, such that the best protected class will be the worst. One could also allow for a switching between SNR-sorting and inverse SNR-sorting depending on the presence of non-stationary noise on the channel.

B. Bit and Power Loading

Figure 5 shows the UEP bit and power loading for the SNR-sorting mode for the defined channel parameters and stationary noise at 512 subcarriers (FFT length 1024), it also shows (with some normalization to fit the given ordinate scale) SER variations according to the different UEP levels. In SNR-sorting, high protected data will be put on low-SNR subcarriers with a correspondingly very low bit load, i.e., small QAM constellations. This ensures a strong protection against non-stationary noise and varying channel conditions. Due to the low bit-load and the resulting data spread over a large number of subcarriers in the highest protected class, narrow-band interference will only hit a few of these carriers, which carry only a few bits. Figure 6 shows the opposite case 'inverse SNR-sorting'. Unlike the SNR-sorting scheme, the high protected data will be placed in the high-SNR subcarriers, but with a correspondingly very high bit-load. Consequently, this concentrates the important data in a few subcarriers. Certainly, this would make the system vulnerable to impulse noise or other non-stationary environments, although it will improve the subcarrier usage.

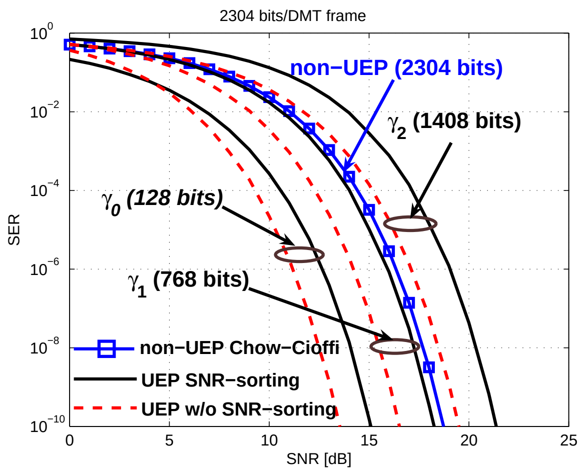

Fig. 3. The SER performance for UEP bit allocation with SNR-sorting, inverse SNR-sorting, and the non-UEP performance for a total target bit rate of 2304 bits per DMT symbol with 512 data carriers (DMT with an FFT-size of 1024) under T1/HDSL NEXT

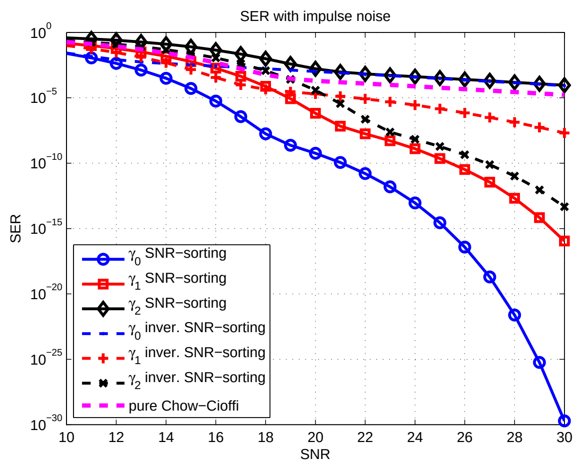

Fig. 4. The SER performance for UEP bit allocation with SNR-sorting, without SNR-sorting, and the non-UEP performance for a total target bit rate of 2304 bits per DMT symbol with 511 data carriers with real measured impulse noise as an additional disturber (bit allocation with T1/HDSL NEXT, only)

VI. Conclusions

We described a UEP bit-allocation scheme as a modification of an earlier non-UEP algorithm by Chow et al.. This allows arbitrary margin definitions according to bit

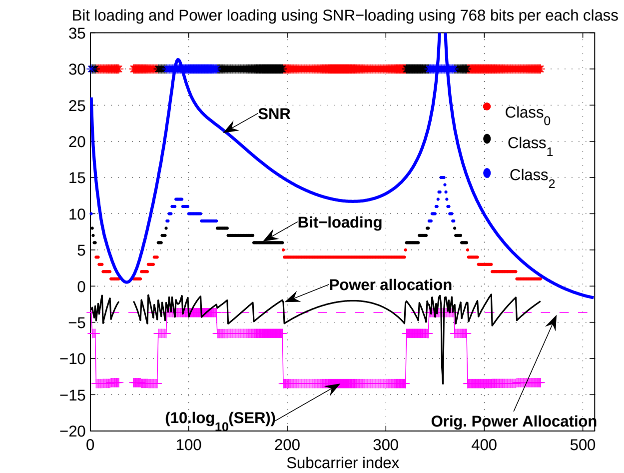

Fig. 5. SNR-sorting bit loading results for ADSL2+ DMT with 512 carriers using a MAR model for an Austrian 0.4-mm cable of 2 km length and T1/HDSL NEXT disturbers

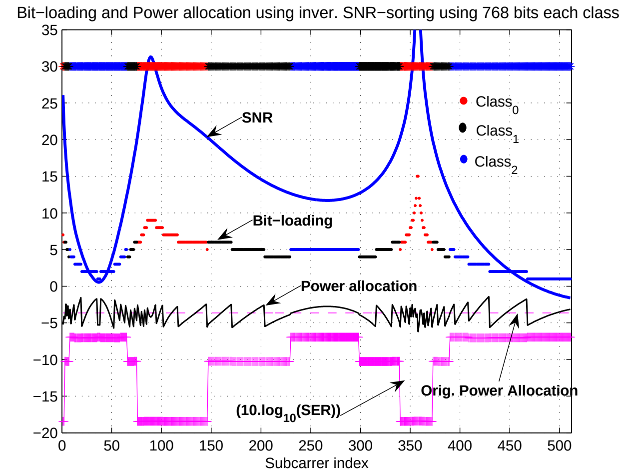

Fig. 6. inverse SNR-sorting bit loading result for VDSL DMT with 1024 carriers using a MAR model for an Austrian 0.4-mm cable of 2 km length and T1/HDSL NEXT disturbers

streams of different priorities. It further allows to devote an arbitrary number of bits to these classes. SNR-sorting will ensure that the high-priority class will still be well protected even under non-stationary noise conditions. This results in somewhat worse performance under stationary conditions although the performance of non-stationary conditions is encouraging. Possible modifications for improving the SNR-sorting scheme were pointed out.

References

[1] **Hughes-Hartogs, D.**, "Ensemble Modem Structure for Imperfect Transmission Media," *U.S. Patents*, Nos. 4,679,227 (July 1987); 4,731,816 (March, 1988); and 4,833,706 (May 1989).

[2] **Campello, J.**, "Practical Bit Loading for DMT," proc. *ICC*, Vancouver, 1999, pp. 801-805.

[3] **Chow, P.S., Cioffi, J.M., Bingham, J.A.C.**, "A practical discrete multitone transceiver loading algorithm for data transmission over spectrally shaped channels," *IEEE Transactions on Communications*, Vol. 43, No. 234, Feb-Mar-Apr 1995, pp. 773 - 775.

[4] **Fischer, R.F.H., Huber, J.B.**, "A New Loading Algorithm for Discrete Multitone Transmission," proc. *Globecom 1996*, Vol. 1, Nov. 18-22, 1996, pp. 724 - 728.

[5] **Yu, F., Willson, A.**, "A DMT transceiver loading algorithm for data transmission with unequal priority over band-limited channels," proc. *Signals, Systems, and Computers, 1999*, Pacific Grove, CA, USA, Vol. 1, Oct. 24-27, 1999, pp. 685 - 689.

[6] **Proakis, J.G.**, *Digital Communications*, 4^{th} Ed., McGraw-Hill, New York, 2001.

[7] "Asymmetric Digital Subscriber Line (ADSL) Transceiver Extended Bandwidth ADSL2 (ADSL2plus),", *ITU-T*, Recommendation G.992.5 (May 2003)

[8] **Musson, J.**, "Maximum likelihood parameters of pair cables", *ETSI TM6*, Madrid, Jan. 1998, TD8, 981t08a1

[9] **Heylen, L., Musson, J.**, "Cable Models Predict Physically Impossible Behaviour in Time Domain," *ETSI TM6*, Plenary No. 16, Amsterdam, Nov. 29 - Dec. 3, 1999

[10] **Tzannes, M.**, "Test Procedure for Digital Subscriber Line (DSL) Transceiver," *ITU-T*, Draft Recommendation G.996.1, Geneva, Switzerland, Oct. 12-23, 2000

[11] **Henkel, W., Kessler, T.**, "A Wideband Impulsive Noise Survey in the German Telephone Netwerk - Statistical Description and Modeling," *AEÜ*, Vol. 48, No. 6, pp. 277-288, Nov./Dec. 1994.

Appendix A

Binary Search Algorithm

The iterative process to find the exact set $\mathcal{M}_j$ is performed by a binary search as follows

1) reset the class counter j to zero
2) find the number of bits in the set $\mathcal{M}_j$
3) if $\sum_k \hat{b}_{k,j} > T_j$, divide the set $\mathcal{M}_j$ to half and move the threshold to these indices, then go to 2).
4) else if $\sum_k \hat{b}_{k,j} < T_j$, divide the next $N_g - 1 - j$ classes into half and move the thresholds to these indices, then go to 2)
5) if T_j is fulfilled, the remaining subcarriers are equally divided among the remaining $N_g - 1 - j$ classes. Increment j by one and go again to 2).

Notes: The number of bits in the last set, $\mathcal{M}_{N_g-1}$, is allowed to vary such that B_T is fulfilled.

Appendix B

Symbol-Error Rate

As in [6], the symbol-error rate equation of $\sqrt{M}$ary pulse amplitude modulation (PAM) is

$$\mathcal{P}^e_{\sqrt{M}} = \left(1 - \frac{1}{\sqrt{M}}\right) \operatorname{erfc}\left(\sqrt{\frac{3}{2(M-1)} \frac{\overline{P}_{k,j}}{N_{k,j}}}\right) , \quad (8)$$

where $M = 2^{b_{k,j}}$. $\overline{P}_{k,j}$ and $N_{k,j}$ are the average signal and noise energies, respectively. Then, for Mary QAM

$$\mathcal{P}^e_M = 1 - \left(1 - \mathcal{P}^e_{\sqrt{M}}\right)^2 = 1 - \left[1 - 2 \cdot \mathcal{P}^e_{\sqrt{M}} + {\mathcal{P}^e_{\sqrt{M}}}^2\right] \quad (9)$$

and from (4), we obtain

$$\mathrm{SNR}_{k,j} = \gamma_j \cdot \left(2^{b_{k,j}} - 1\right) . \quad (10)$$

Using (10) inside (8) and $M = 2^{\hat{b}_{k,j}}$,

$$\mathcal{P}^e_{\sqrt{M}} = \left(1 - \frac{1}{\sqrt{2^{\hat{b}_{k,j}}}}\right) \operatorname{erfc}\left(\sqrt{\frac{3\gamma_j}{2}}\right) . \quad (11)$$

Equation (9) and (11) lead to the desired symbol-error relation relation (5)